Regularisation of the equivalent source method for robust numerical modelling of acoustic scattering

Bhan Lam[a]
Digital Signal Processing Laboratory, School of Electrical and Electronic Engineering, Nanyang Technological University
S2-B4a-03, 50 Nanyang Avenue, 639798, Singapore

Stephen Elliott[b]
Jordan Cheer[c]
Institute of Sound and Vibration Research, University of Southampton
Engineering and the Environment, University of Southampton, Southampton SO17 1BJ, United Kingdom

Woon-Seng Gan[d]
Digital Signal Processing Laboratory, School of Electrical and Electronic Engineering, Nanyang Technological University
S2-B4a-03, 50 Nanyang Avenue, 639798, Singapore

The equivalent source method can be used to model acoustic scattering, by representing the scattering object with a set of equivalent sources that satisfy a boundary condition. The equivalent source strengths are optimised by a least-squares method. When the equivalent sources are positioned further from the boundary to reduce the boundary condition error, the optimisation becomes ill-conditioned. This limits the application of the equivalent source method in irregularly-shaped objects as boundary condition error is highly sensitive to equivalent source placement. To overcome the problem of ill-conditioning, a regularisation parameter is introduced, which increases the robustness to errors in the modelled acoustic field by limiting the power of overdriven equivalent sources. Simulations of a rigid infinite wall with an equivalent dipole line-array, reveal that regularisation reduces boundary condition error in all ill-conditioned cases. Good trade-offs between boundary condition error and regularisation are achieved for a wide range of

[a] email: blam002@e.ntu.edu.sg
[b] email: s.j.elliott@soton.ac.uk
[c] email: j.cheer@soton.ac.uk
[d] email: ewsgan@ntu.edu.sg

regularisation parameter values. This allows the results to be calculated for varying frequencies and distances between the equivalent sources and the boundary. Regularisation reduces the sensitivity of boundary condition error to equivalent source placement, thereby increasing the flexibility of the equivalent source method for irregularly-shaped scattering objects.

1   INTRODUCTION

Numerical modelling techniques have been widely used to solve radiation and scattering problems, and are able to provide a visual analysis of a complex sound field. These techniques such as the finite element (FE) method, boundary element method (BEM), and increasingly, the wave superposition or equivalent source method (ESM), each have their own merits depending on the type of boundary conditions specified.

The FE method is not primarily suited for free-field modelling due to a large number of elements involved in the 'infinite' domain[1]. BEM, has one less computational dimension than FE, increasing its computational efficiency, and thus well suited for an infinite domain. The drawbacks of BEM, however, are non-unique solutions at some eigen-frequencies and singularities at the boundaries[1-3]. An alternative boundary-based method for free-field radiation, originally called the wave superposition method[2, 4-6] by Koopmann et al, possesses unique merits over BEM. Key advantages of the superposition method include: (1) increased computational efficiency over BEM and FE[1], (2) Non-uniqueness and singularities are avoided as equivalent sources are placed a distance away from the boundary instead of on the boundary in BEM.

The principles of the wave superposition method have also been known by others in the literature such as the method of fundamental solutions[3], and more commonly, the equivalent source method (ESM)[1, 7-17]. Applications of the ESM have expanded to areas in near-field acoustic holography[7, 9, 17], aeroacoustics[13-15], and acoustic scattering in general[1, 3, 10-12].

In a radiation problem, the ESM replaces the radiator with an array of virtual point sources (within the radiator) that emulate the normal particle velocity distribution on the boundary according to the initial radiation conditions. Similarly, acoustic scattering is simulated by replacing a scattering object by an array of point sources within the boundary, driven to achieve the desired boundary condition (e.g., rigid wall).

ESM is commonly formulated either by the least-squares method[4] (LSM) or the full-field equation[18] (FFE) approach. The FFE method was developed to alleviate the ill-conditioning due to singular value decomposition in the LSM. Performance comparisons[10], however, show that LSM is more precise than FFE especially at low frequencies, which are an area of interest to active noise control (ANC) systems (ANC systems are most effective at low frequencies). The ill-conditioning problem of LSM results in high sensitivity to source placement, number of sources and wavenumber, narrowing the modelling capabilities of the ESM.

However, the LSM can be 'regularised' by a weighting parameter to provide a robust optimal solution with minimal increase in the mean-square-error[19, 20]. We demonstrate that the introduction of a regularisation parameter ensures that the solution of LSM is always well-conditioned, significantly improving its stability.

2   THEORY

An acoustic wave will perfectly reflect off an infinite wall with rigid boundary conditions (zero normal velocity). By emulating this scenario, the effect of regularisation can be investigated and the results compared with an analytical model using image sources.

The rigid wall can be represented by an equivalent set of dipole sources in one dimension. This represents a slight modification to the use of dipoles in the active control of noise in a duct[21], which generates an upstream, or reflected wave of twice the amplitude and terminates the propagating wave downstream (perfect reflection) in one dimension.

By analogy with the one-dimensional case and also as suggested by Gounot and Musafir[11], an equivalent dipole line source approach can be adopted for two dimensions.

2.1 Free-field Equations

The complex pressure fluctuation due to a point source at a radial distance r is

$$p(r) = \frac{j\omega\rho_0 e^{-jkr}}{4\pi r},$$ (1)

and the complex radial velocity due to the point source is given by

$$u_r(r) = \frac{q}{4\pi}\left(\frac{jk}{r} + \frac{1}{r^2}\right)e^{-jkr},$$ (2)

where ω is the angular frequency, ρ_0 is the density of air, k is the wavenumber, and q is the complex source strength of the point source in terms of volume velocity.

2.2 Matrix Formulation of the Equivalent Source Method (ESM)

The complex normal velocity field, $\mathbf{u}$, on a boundary can be evaluated by summing the contributions of the primary disturbance and the internal equivalent sources at evaluation points on the boundaries at $x = D$ and $x = F$, which represent the two sides of the infinite wall. $\mathbf{u}$ is a complex vector that can be expressed in matrix form as

$$\mathbf{u} = \mathbf{u}_p + \mathbf{u}_{int},$$ (3)

where $\mathbf{u}_p$ is an $N \times 1$ complex vector corresponding to the velocity at the N evaluation points due to the primary source and is given by

$$\mathbf{u}_p = \left[\frac{A}{j\omega\rho_0}\left(\frac{jk}{r_{p,1}} + \frac{1}{r_{p,1}^2}\right)e^{-jkr_{p,1}}\cos\theta_{p,1} \cdots \frac{A}{j\omega\rho_0}\left(\frac{jk}{r_{p,N}} + \frac{1}{r_{p,N}^2}\right)e^{-jkr_{p,N}}\cos\theta_{p,N}\right]^T.$$ (4)

$r_{p,N}$ represents the distance from the primary source location to the N th evaluation point; $\theta_{p,N}$ is the angle formed between the primary source and the N th evaluation point; A is the complex amplitude of the primary source; and T is the transpose operator.

The normal velocity contribution from the M internal equivalent sources at the evaluation points, $\mathbf{u}_{int}$, is expressed with a $N \times M$ transform matrix, $\mathbf{T}_e$, as

$$\mathbf{u}_{int} = \mathbf{T}_e \mathbf{q}_{int},\tag{5}$$

where $\mathbf{q}_{int} = [q_1 \ldots q_M]^T$ is an $M \times 1$ complex vector of internal volume velocities. The transform matrix $\mathbf{T}_e$ takes into account the reverse direction (normal primary velocity on the boundary) to emulate a rigid wall ($\mathbf{u} = 0$) condition for perfect reflection of the wave at $x = D$ for a primary source located at $(0,0)$, and is expressed as

$$\mathbf{T}_e = \frac{1}{4\pi} \begin{pmatrix} -\left(\dfrac{jk}{r_{1,1}} + \dfrac{1}{r_{1,1}^2}\right) e^{-jkr_{1,1}} \cos\theta_{1,1} & \cdots & -\left(\dfrac{jk}{r_{M,1}} + \dfrac{1}{r_{M,1}^2}\right) e^{-jkr_{M,1}} \cos\theta_{M,1} \\ \vdots & \ddots & \vdots \\ -\left(\dfrac{jk}{r_{1,\frac{N}{2}}} + \dfrac{1}{r_{1,\frac{N}{2}}^2}\right) e^{-jkr_{1,\frac{N}{2}}} \cos\theta_{1,\frac{N}{2}} & \cdots & -\left(\dfrac{jk}{r_{M,\frac{N}{2}}} + \dfrac{1}{r_{M,\frac{N}{2}}^2}\right) e^{-jkr_{M,\frac{N}{2}}} \cos\theta_{M,\frac{N}{2}} \\ \left(\dfrac{jk}{r_{1,\frac{N}{2}+1}} + \dfrac{1}{r_{1,\frac{N}{2}+1}^2}\right) e^{-jkr_{1,\frac{N}{2}+1}} \cos\theta_{1,\frac{N}{2}+1} & \cdots & \left(\dfrac{jk}{r_{M,\frac{N}{2}+1}} + \dfrac{1}{r_{M,\frac{N}{2}+1}^2}\right) e^{-jkr_{M,\frac{N}{2}+1}} \cos\theta_{M,\frac{N}{2}+1} \\ \vdots & \ddots & \vdots \\ \left(\dfrac{jk}{r_{1,N}} + \dfrac{1}{r_{1,N}^2}\right) e^{-jkr_{1,N}} \cos\theta_{1,N} & \cdots & \left(\dfrac{jk}{r_{M,N}} + \dfrac{1}{r_{M,N}^2}\right) e^{-jkr_{M,N}} \cos\theta_{M,N} \end{pmatrix}.\tag{6}$$

Similar to Eqn. (4), $r_{M,N}$ represents the distance between the M th internal equivalent source and the N th evaluation point on the boundary. $\theta_{M,N}$ is the angle between the M th equivalent source and the N th evaluation point. For values in $\mathbf{T}_e$ from 1 to $N/2$ (top half), an additional negative sign is added to indicate an inversion in direction of normal velocity on the boundary at $x = D$.

2.3 Regularisation

With a rigid boundary condition, and incorporating Eqn. (5) into Eqn. (3), the optimal equivalent complex source strengths can be evaluated by a least-squares approach given by

$$\mathbf{q}_{int} = -\left(\mathbf{T}_e\right)^{-1} \mathbf{u}_p.\tag{7}$$

Taking into account that $\mathbf{T}_e$ is not a square matrix, a Moore-Penrose pseudoinverse form is adopted as

$$\mathbf{q}_{int} = -\left(\mathbf{T}_e^H \mathbf{T}_e + \beta \mathbf{I}\right)^{-1} \mathbf{T}_e^H \mathbf{u}_p,\tag{8}$$

where $\mathbf{I}$ is an $N \times N$ identity matrix and β is a regularisation parameter that is added to regularise[19] the $\mathbf{T}_e^H \mathbf{T}_e$ matrix to prevent it from being ill-conditioned during inversion. H is defined as the conjugate transpose.

2.4 Error and Difference Index

A normalised error criterion, E, at all evaluation points on the boundaries, is minimised based on Eqn. (8) and is evaluated by

$$E = 10 \log_{10} \left(\frac{\mathbf{u}^H \mathbf{u}}{\mathbf{u}_p^H \mathbf{u}_p} \right). \tag{9}$$

To discount the effects of inaccuracies expected at the end of the 'infinite' wall, another error criterion, E' is defined as

$$E' = 10 \log_{10} \left(\frac{\mathbf{u}_{2\lambda}^H \mathbf{u}_{2\lambda}}{\mathbf{u}_{p,2\lambda}^H \mathbf{u}_{p,2\lambda}} \right), \tag{10}$$

where $\mathbf{u}_{2\lambda}$ and $\mathbf{u}_{p,2\lambda}$ represent, in order, the total and primary normal velocities on the wall boundary at $x = D$ and $x = F$ bounded by the 2λ zone shown in Fig. 1.
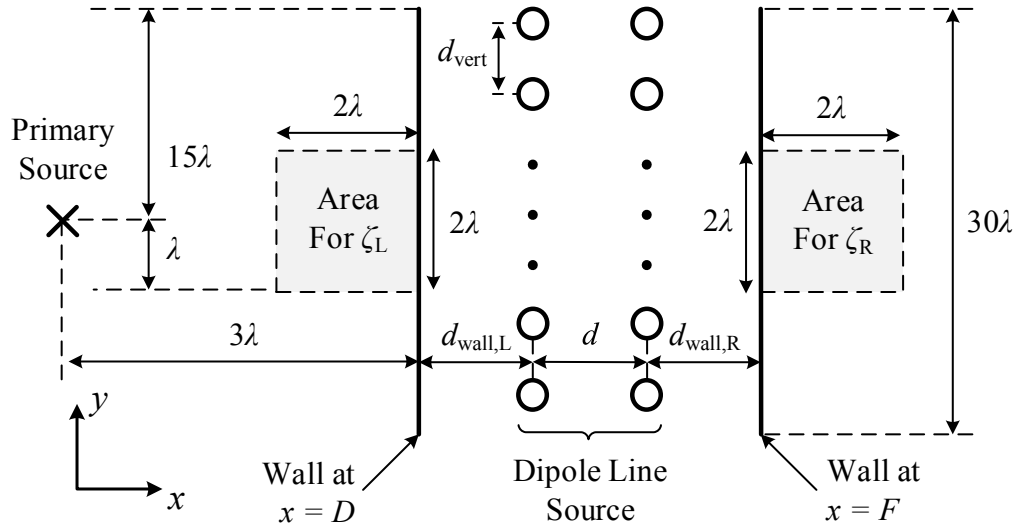

Fig. 1 – Parameters associated with the arrangement of the dipole line source; location of the $2\lambda \times 2\lambda$ area used in calculation of ζ_L and ζ_R; dimensions of the wall; and the primary disturbance source location in the x-y plane.

The pressure in the computation plane is the real part of the total pressure due to the sum of primary and equivalent sources, $p(r)$, multiplied by $e^{j\omega t}$ when $t = 0$, and is expressed as

$$p(r) = p_p(r) + \sum_{l=1}^{M} p_{int,l}(r), \tag{11}$$

where $p_p(r)$ is the pressure at radial distance r due to the primary source and $p_{int,l}(r) = \left[j\omega q_{int,l} e^{-jkr} / 4\pi r \right]$ is the complex pressure fluctuation at r from the lth internal equivalent source ($l \in \mathbb{C}^+$ from 1 to M).

The accuracy of the equivalent source method can be evaluated by comparing the difference between the reflection pattern in an area near the rigid boundary with that calculated analytically using the image of the primary sound source. A combined sound field of the primary source and its image (located at 6λ or $2D$ in the positive x direction) is set up as shown in Fig. 2.
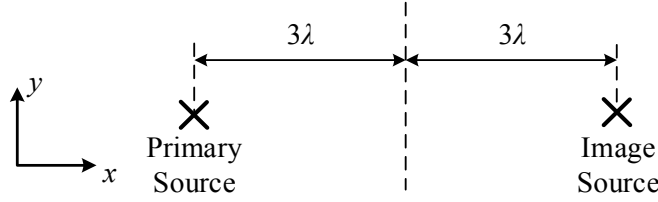

Fig. 2 – Primary source and its image.

The difference between the desired sound field due to the primary and its image source (perfect reflection) and the sound field produced by the equivalent sources method is expressed by a difference index, ζ_L, over the left-hand $2\lambda \times 2\lambda$ region shown in Fig. 1 as

$$\zeta_L = 10 \log_{10} \left(\frac{\sum_{l=1}^{i} \left| p_{image}(r_l) - p(r_l) \right|^2}{\sum_{l=1}^{i} \left| p_{image}(r_l) \right|^2} \right), \tag{12}$$

where i is the total number of points in the area as defined by the left-hand $2\lambda \times 2\lambda$ area in Fig. 1; r_l is the radial distance to the lth position in the $2\lambda \times 2\lambda$ evaluation area; $p_{image}(r_l)$ is the complex pressure calculated using the image source model at r_l; and $p(r_l)$ is the pressure due to the equivalent source model at r_l.

To evaluate the attenuation 'behind' the wall, another difference index, ζ_R, is defined with relation to the sum-square pressures due to $p_{image}(r_l)$ of the left-hand $2\lambda \times 2\lambda$ evaluation area as

$$\zeta_R = 10 \log_{10} \left(\frac{\sum_{l=1}^{v} \left| p(r_l) \right|^2}{\sum_{l=1}^{i} \left| p_{image}(r_l) \right|^2} \right), \tag{13}$$

where i and v is the total number of points in left-hand and right-hand $2\lambda \times 2\lambda$ area in Fig. 1, respectively.

3   RESULTS

The primary point source is located at the origin with the initial sound pressure $|A|$ fixed at 90 dB (ref. 20 μPa). From Fig. 1, the rigid boundary nearest to the primary source is located at $x = D$, and is set as 3λ. The horizontal separation of the dipoles, d; the vertical separation of the dipoles, d_{vert}; the distance between the left boundary and the dipole, $d_{wall,L}$; and the distance between the right boundary and the dipole, $d_{wall,R}$, are illustrated in Fig. 1. To simulate an 'infinite' wall, the height of the wall is at least 15λ above and below the x-axis for a primary source located at the origin.

3.1 Equivalent Source Positions

For a dipole source to radiate in only one direction (in one dimension), the separation distance, d, has to be small compared to the wavelength[21]. As a general guideline, $d < \lambda/10$ can yield close to zero downstream radiation. Thus, d is fixed at $\lambda/10$.

The total number of equivalent sources is determined by the total height of the wall at 30λ and the separation between the sources, $d = d_{vert} = \lambda/10$. The ratio of evaluation points on the boundary to the number of equivalent sources is fixed at 16 to ensure an accurate reconstruction of the velocity at the boundary.

The stability of the equivalent source method (ESM) solution is particularly sensitive to the distance between the boundary and the equivalent sources within the scattering/radiating object[22]. By varying the width of the wall, $w = d_{wall,L} + d + d_{wall,R}$, the ability of the regularisation parameter, β, to yield stable ESM solutions can be evaluated.

The pressure field of a perfect reflection produced by the analytical image source model is shown in Fig. 3. Visual comparison of the pressure field using the ESM for $kw = 0.03$ in Fig. 4 with the analytical solution in Fig. 3, illustrates the inability of ESM to reproduce an accurate pressure field for low kw. For higher kw, ESM is able to reproduce a visually similar pressure distribution to the analytical solution from comparison of Fig. 3 and Fig. 4(b).
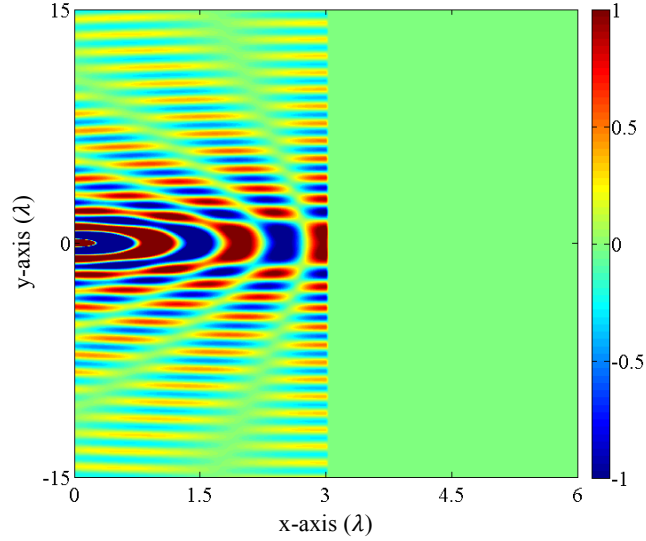
Fig. 3 – Pressure plot of reflection of an 'infinite' wall at 3λ using the image source method.
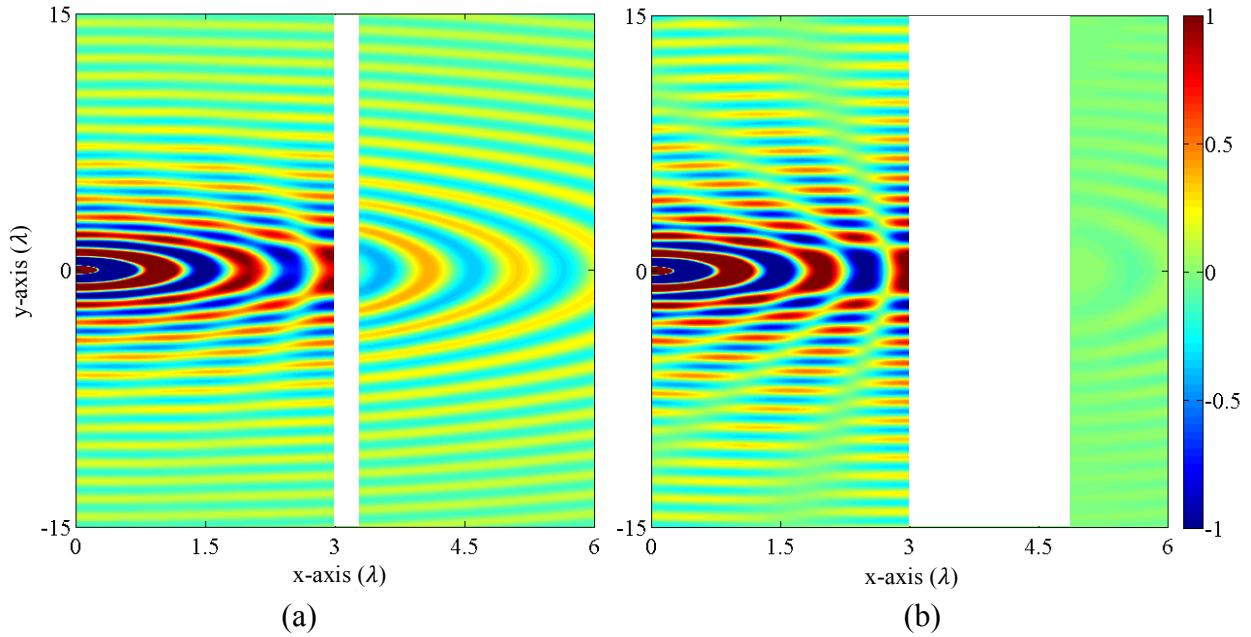

(a) (b)

Fig. 4 – Pressure field using the equivalent source method to simulate an 'infinite' wall for (a) $kw = 0.03$ and (b) $kw = 0.22$, without regularisation.

3.2 Effect of β on Boundary Error

In order to prevent β from overcompensating, resulting in inaccuracies, the value of β should be carefully chosen. A wide of range of β values were tested to illustrate the effects of overcompensation when the magnitude of β is too large, as shown in Fig. 5(a).

As kw increases, the velocity reconstruction at the boundary improves, yielding low boundary error values. At higher values of kw however, ill-conditioning during matrix inversion results in poor reconstruction, shown by the high boundary error values when $\beta = 0$.

Introduction of small values of β significantly reduces the boundary error for $kw > 0.11$ as shown in Fig. 5(b). For the values of kw tested, β values in the range from 10^{-9} to 10^{-5} provide a substantial improvement for the ill-conditioned cases ($kw > 0.11$) without affecting the performance of well-conditioned ($kw < 0.13$) cases.
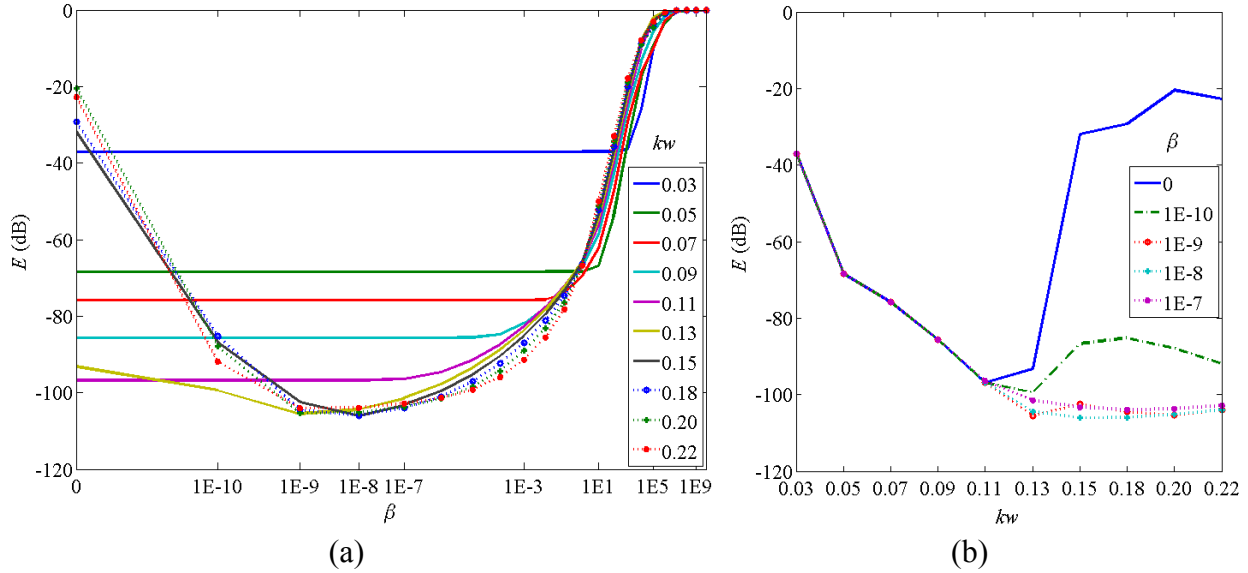

(a)   (b)

Fig. 5 – (a) Boundary error over the whole width of the wall, E, for increasing values of β at different kw. (b) Effect of β on boundary error E as kw increases.

Evaluating the boundary error, E', within the 2λ zone depicted in Fig. 1, a similar increase in error due to ill-conditioning occurs for $kw > 0.11$, as shown in Fig. 6(a). The improvement in E', due to introduction of β values in the range from 10^{-9} to 10^{-5}, is still evident as highlighted in Fig. 6(b). The similar improvements in the boundary error for both E and E' show that ill-conditioning results in inaccuraciesAN across the entire length of the boundaries.
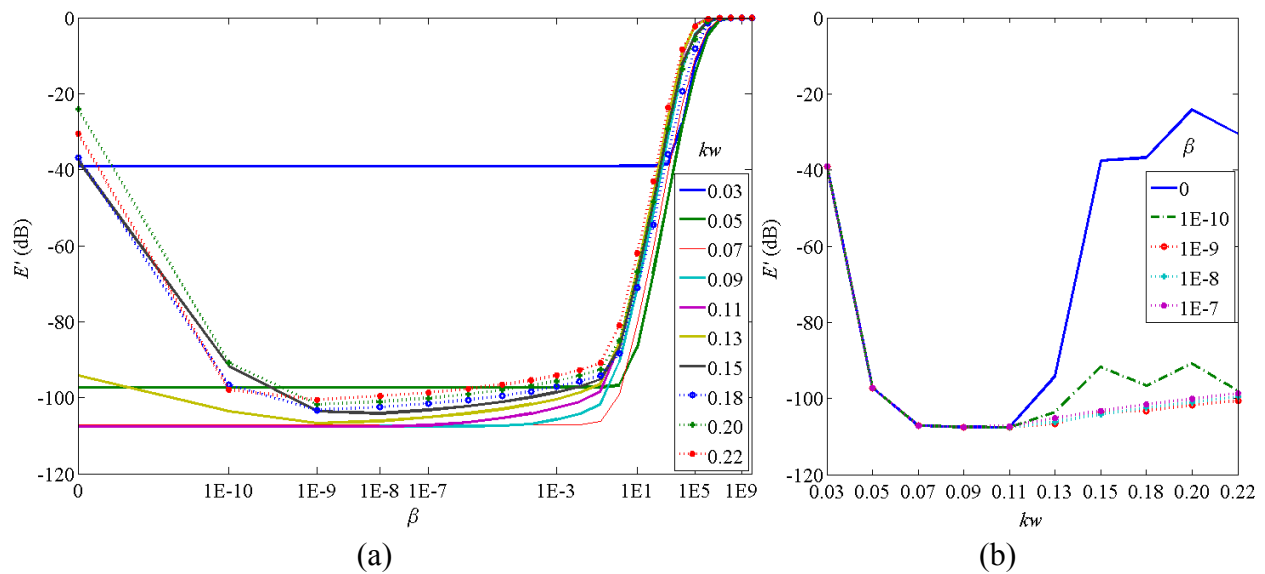

(a)   (b)

Fig. 6 - (a) Boundary error within the 2λ zone, E', for increasing magnitude of β at different kw. (b) Effect of β on boundary error E' as kw increases.

3.3 Effect of β on Difference Index, ζ_L and ζ_R

For the equivalent source method (ESM) to radiate/scatter accurately, it should also produce pressure fields that are also the same as the analytical solution. The normalised difference in sum-square pressures between the analytical solution (e.g., perfect reflection) and the ESM is defined in Eqn. (12) as ζ_L. Since lower values (in dB) of ζ_L indicate less difference between ESM and the analytical solution, it can be seen from Fig. 7(a) that as kw increases, ζ_L decreases.

The normalised sum-square pressures in the $2\lambda \times 2\lambda$ zone after the wall, where no wave propagation is expected, is defined in Eqn. (13) as ζ_R. The trend is consistent with ζ_L as ζ_R is also inversely proportional to kw according to Fig. 7(b).

Analysis of Fig. 7 shows that the introduction of β has no impact on the radiation pattern of ESM provided that the value of β is less than about 10, which is the value for which the boundary error is not increased in Fig. 6. Even though high boundary errors due to ill-conditioning did not translate into spurious radiation in the studied zone, spurious radiation has been observed near the edges of the 'infinite' wall. Therefore, ill-conditioning will cause inaccuracies in radiation/scattering under certain scenarios.
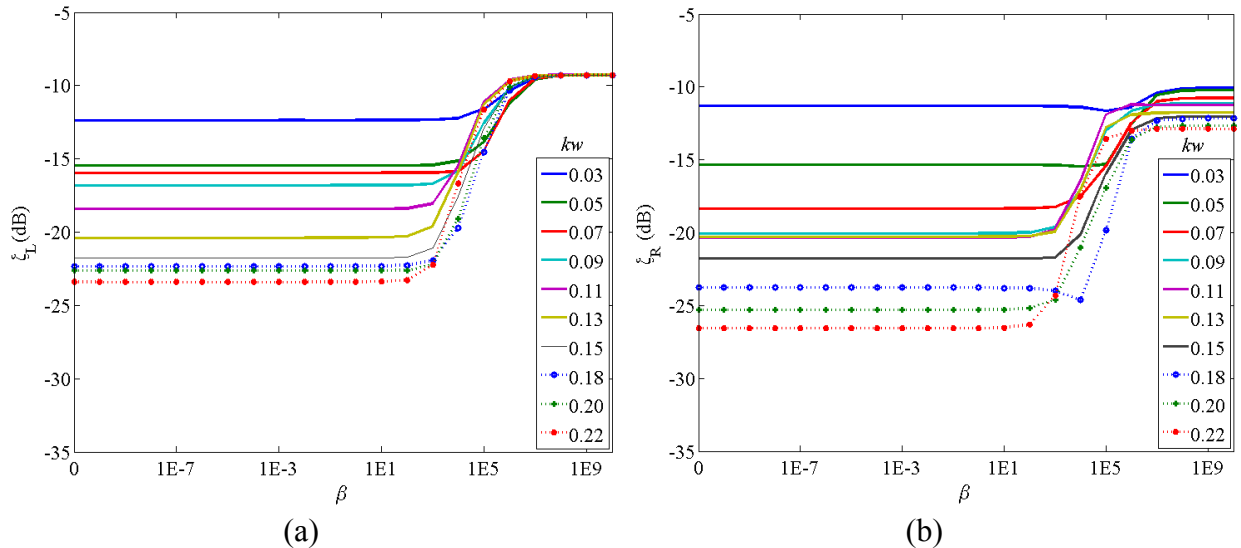

(a) (b)

Fig. 7 – (a) Effect of β on the difference index, ζ_L, in the left-hand zone. (b) Effect of β on the difference index, ζ_R, in the right-hand zone.

4 DISCUSSION AND CONCLUSIONS

The equivalent source method (ESM) can be used to study acoustic scattering by driving an array of equivalent sources to match the desired boundary condition of the scattering/radiating object. ESM can be solved either by the least-squares or full-field equation approach with the former yielding higher accuracy in the low frequency region. Low frequencies are an area of interest for active noise control (ANC) applications as ANC operates most effectively at such frequencies.

The matrix formulation of the least-squares method brings about an inherent conditioning problem due to matrix inversion. Introduction of a regularisation parameter, β, has been shown

to significantly mitigate the errors introduced by ill-conditioning without affecting cases where the problem is well-conditioned.

Regularisation of ESM has demonstrated improvements in reducing boundary reconstruction error of the surface velocity. However, the sound field radiation accuracy is ultimately dependent on the frequency-dependent distance between the boundary and the embedded equivalent sources, and appears to be less affected by the ill-conditioning that is compensated by regularisation.

5 ACKNOWLEDGEMENTS

6 REFERENCES

1. M. Johnson, S. Elliott, K. Baek and J. Garcia-Bonito, "An equivalent source technique for calculating the sound field inside an enclosure containing scattering objects", J. Acoust. Soc. Am., **104** (3), 1221-1231, (1998).

2. A. Leblanc, R. K. Ing and A. Lavie, "A Wave Superposition Method Based on Monopole Sources with Unique Solution for All Wave Numbers", Acta Acust united Ac, **96** (1), 125-130, (2010).

3. G. Fairweather, A. Karageorghis and P. A. Martin, "The method of fundamental solutions for scattering and radiation problems", Eng Anal Bound Elem, **27** (7), 759-769, (2003).

4. G. H. Koopmann, L. Song and J. B. Fahnline, "A method for computing acoustic fields based on the principle of wave superposition", J. Acoust. Soc. Am., **86** (6), 2433-2438, (1989).

5. L. Song, G. H. Koopmann and J. B. Fahnline, "Numerical errors associated with the method of superposition for computing acoustic fields", J. Acoust. Soc. Am., **89** (6), 2625-2633, (1991).

6. J. B. Fahnline and G. H. Koopmann, "A numerical solution for the general radiation problem based on the combined methods of superposition and singular-value decomposition", J. Acoust. Soc. Am., **90** (5), 2808-2819, (1991).

7. M. R. Bai, C.-C. Chen and J.-H. Lin, "On optimal retreat distance for the equivalent source method-based nearfield acoustical holography", J. Acoust. Soc. Am., **129** (3), 1407-1416, (2011).

8. C.-X. Bi and J. S. Bolton, "An equivalent source technique for recovering the free sound field in a noisy environment", J. Acoust. Soc. Am., **131** (2), 1260-1270, (2012).

9. C.-X. Bi, X.-Z. Chen and J. Chen, "Sound field separation technique based on equivalent source method and its application in nearfield acoustic holography", J. Acoust. Soc. Am., **123** (3), 1472-1478, (2008).

10. Y. Gounot, R. E. Musafir and J. G. Slama, "A comparative study of two variants of the equivalent sources method in scattering problems", Acta Acust united Ac, **91** (5), 860-872, (2005).

11. Y. J. Gounot and R. E. Musafir, "On appropriate equivalent monopole sets for rigid body scattering problems", J. Acoust. Soc. Am., **122** (6), 3195-3205, (2007).

12. Y. J. Gounot and R. E. Musafir, "Simulation of scattered fields: some guidelines for the equivalent source method", JSV, **330** (15), 3698-3709, (2011).

13. F. Holste, "An equivalent source method for calculation of the sound radiated from aircraft engines", JSV, **203** (4), 667-695, (1997).

14. S. Lee, K. S. Brentner and P. J. Morris, "Acoustic scattering in the time domain using an equivalent source method", AIAA journal, **48** (12), 2772-2780, (2010).

15. S. Lee, K. S. Brentner and P. J. Morris, "Assessment of time-domain equivalent source method for acoustic scattering", AIAA journal, **49** (9), 1897-1906, (2011).

16. R. Piscoya, H. Brick, M. Ochmann and P. Költzsch, "Equivalent source method and boundary element method for calculating combustion noise", Acta Acust united Ac, **94** (4), 514-527, (2008).

17. N. P. Valdivia and E. G. Williams, "Study of the comparison of the methods of equivalent sources and boundary element methods for near-field acoustic holography", J. Acoust. Soc. Am., **120** (6), 3694-3705, (2006).

18. M. Ochmann, "The full-field equations for acoustic radiation and scattering", J. Acoust. Soc. Am., **105** (5), 2574-2584, (1999).

19. S. Elliott, *Signal Processing for Active Control*. Academic Press, (2001).

20. M. F. Simón-Gálvez, S. J. Elliott and J. Cheer, "The effect of reverberation on personal audio devices", J. Acoust. Soc. Am., **135** (5), 2654-2663, (2014).

21. P. A. Nelson and S. J. Elliott, *Active control of sound*. Academic Press, (1992).

22. R. Jeans and I. C. Mathews, "The wave superposition method as a robust technique for computing acoustic fields", J. Acoust. Soc. Am., **92** (2), 1156-1166, (1992).